Int. J. of Applied Mechanics and Engineering, 2006, vol.11, No.3, pp.515-527

This paper was prepared on the Fourth International Tribology Conference ITC 2006

FRICTION FORCES FOR HUMAN HIP JOINT LUBRICATION AT A NATURALLY PERMEABLE CARTILAGE

K.Ch. WIERZCHOLSKI*
Tech. Univ. Gdańsk, Faculty of Ocean Eng.& Ship Tech.
Narutowicza 11 PL-80952 Gdańsk
Maritime University Gdynia, PL81-225 Gdynia, POLAND
e-mail: wierzch@am.gdynia

This paper presents various kinds of friction forces occurring in a human joint gap. Some main factors which can change the friction forces in a human joint are indicated. Friction forces for squeezing, boosted squeezing and weeping in macro, micro and nano level for porous cartilage are presented here. According to the author's knowledge the problem of human joint lubrication in unsteady motion has not been hitherto considered in scientific papers on bio-tribology.

Key words: friction forces, porous cartilage, human hip joint.

1. Preliminaries

This paper shows comparisons between friction forces in spherical and other curvilinear orthogonal co-ordinates for hydrodynamic steady and unsteady unsymmetrical synovial non-Newtonian fluid flow with variable viscosity and for random changes of human hip joint gap. Similar comparisons but for constant viscosity of synovial fluid and symmetrical flow only, without numerical calculations, were obtained in earlier analytical papers (Dowson, 1990; Sieroń, 2000; Ahn *et al.*, 2001; Chizhik *et al.*, 1998). According to the author's knowledge the friction forces calculation of human joints in unsteady motion have not been hitherto considered in the scientific papers on biotribology (Ahn *et al.*, 2001; Chizhik *et al.*, 1998; 2004; Mow *et al.*, 1984; 1990; 1991; Mow and Guilak, 1994).

The roughness of cartilage surface has influence on the values of friction forces (Wierzcholski, 2005 a; b; c; d; f; Wierzcholski and Cwanek, 2005e).

Between two cooperating rough cartilage bodies in human bio- joints various kinds of friction effect can be observed. Table 1 presents a diagram of friction mechanisms occurring between two cooperating cartilage surfaces in human joints. Table 1 shows the various kinds of wet and dry frictions occurring in human joints

Table 1. Diagram of friction mechanism between two rough cartilage bodies in bio joint.

* To whom correspondence should be addressed

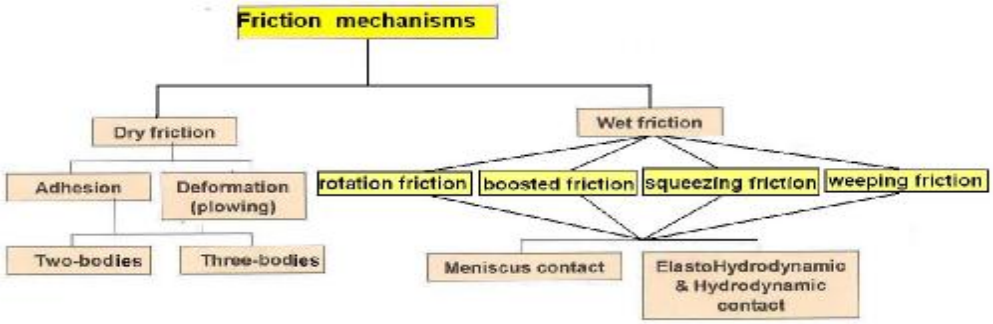

In this paper the friction forces are determined by applying the measured roughness of cartilage surfaces in human joint, cartilage pores of about *6-10 nm* in size, calculated components of synovial fluid velocity and values of hydrodynamic pressure as well.

Friction forces are caused by the adhesion and cohesion (Ahn *et al.*, 2001; Chizhik *et al.*, 1998; 2004).

The proper description of friction forces in bio-joints enables to estimate and determine quantity of wear in human joints.

It is easy to see that a numerical analysis of the synovial fluid flow in joint gap and simultaneous analysis of friction forces and friction coefficients in human hip joints can be possible by using equations of motion and analytical solutions of synovial fluid velocity components.

2. Geometrical and physical data and kinds of measurements

In order to present the problem, in Fig.1 we show hydrodynamic, boosted, squeezing and weeping lubrication in bio-bearing joint. In Fig.1 we use the following notations: 1- articular cartilage, 2-synovial fluid, 3-wedge shaped gap, 4- synovial fluid flow in cartilage matrix, 5- squeezed synovial liquid, 6- non- loaded region of cartilage, 7- loaded region of cartilage. In Fig.1a the geometry of cartilage and synovial fluid flow create a hydrodynamic kind of lubrication.

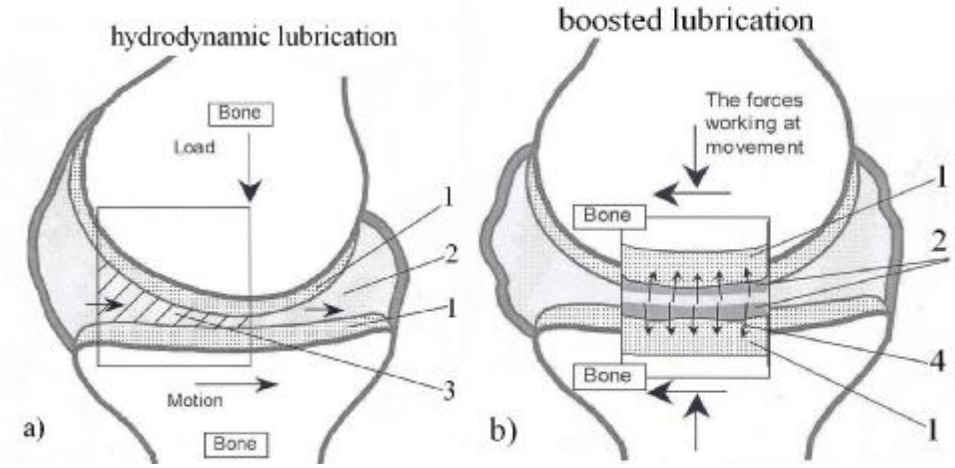

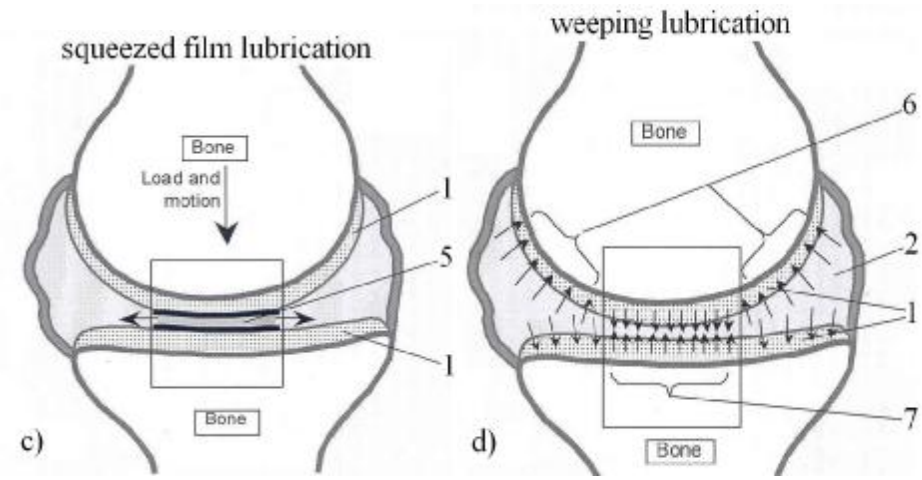

Fig.1. Various kinds of lubrication in bio-bearing: a) hydrodynamic, b) boosted, c) squeezed, d) weeping.

In the boosted lubrication (see Fig.1b) the flow of small molecular elements of synovial fluid in a cartilage pores enables the lubrication of cartilage surface during the joint functioning.

The thickness of squeezed synovial liquid film shown in Fig.1c can achieve dozens of micrometers and separate the cooperating surfaces completely.

In the weeping lubrication presented in Fig.1d, the liquid is moved away from the cartilage and produces the hydrostatic pressure which keeps the surface at the distance some micrometers.

Friction forces in the hydrodynamic lubrication are pointed toward identical horizontal directions (see Fig.2a). Friction forces in the boosted lubrication are in opposite vertical directions pointing outward the gap (see Fig.2b). Friction forces in the squeezing lubrication are in reverse horizontal directions (see Fig.2c). Friction forces in the weeping lubrication are in opposite vertical directions pointing inward the gap and in skew directions pointing outward the gap (see Fig.2d).

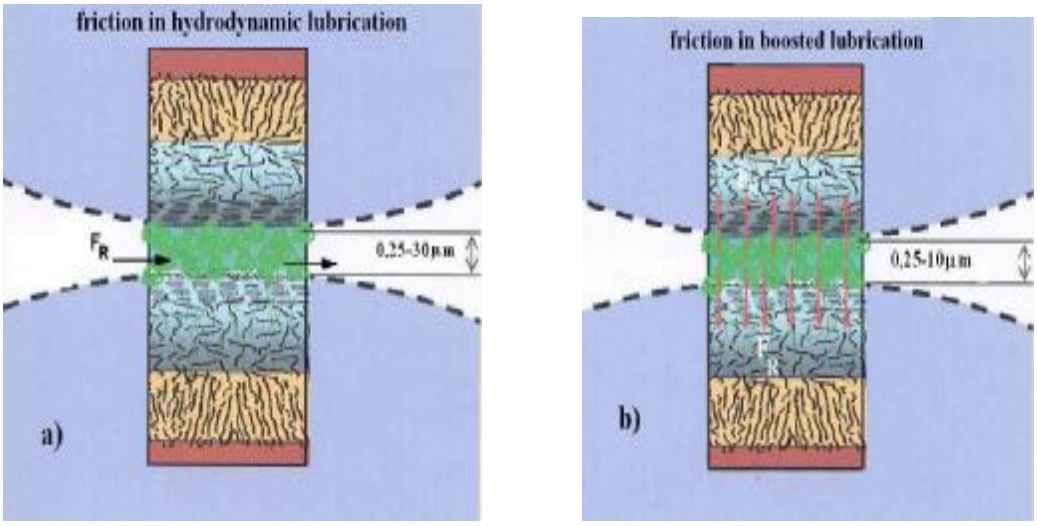

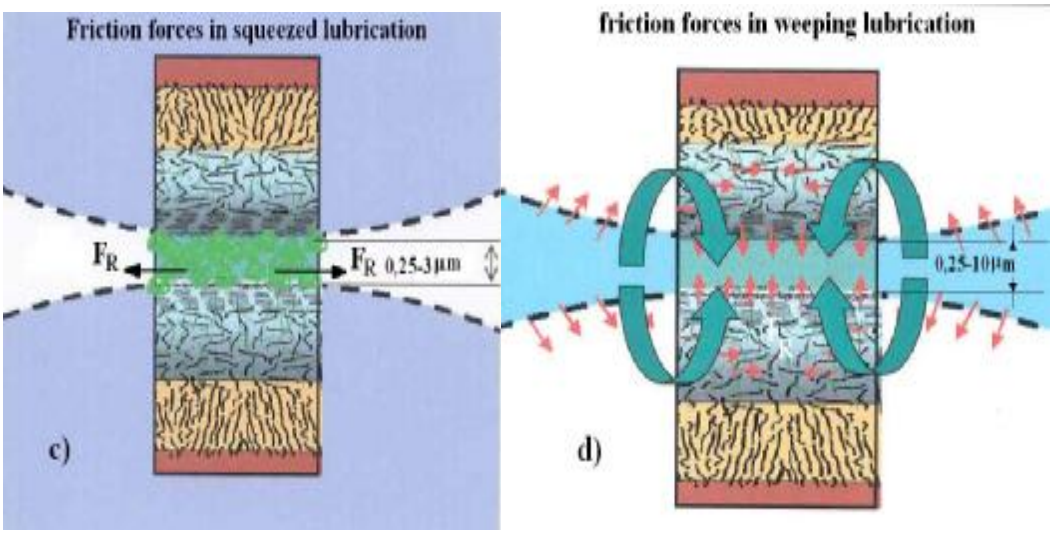

Fig.2. Friction forces in various kinds of lubrication: a) hydrodynamic, b) boosted, c) squeezed, d) weeping.

This paper provides a short description of the acoustic emission method (AE) with respect to orthopedic diagnostics. The application of acoustic emission to surveillance of human knee joint under a typical daily load, is presented. The typical loads comprise knee bending, climbing the stairs, walking, and cycling. In this application the AE transducer is fixed at the medial condyle of the human femur (see Fig.3a; b). Simultaneously with the acoustic emission measurements, flexion measurements of the knee were performed by utilize an inclinometer fixed at the leg of the patient (Fink and Manthei, 2004; Manthei, 2006). The measurements are performed in University of Applied Science in Giessen (Germany) and had been supported by a Marie Curie Transfer of Knowledge Fellowship of the European Community's Sixth Framework Program under contract number MTKD-CT-2004-517226.

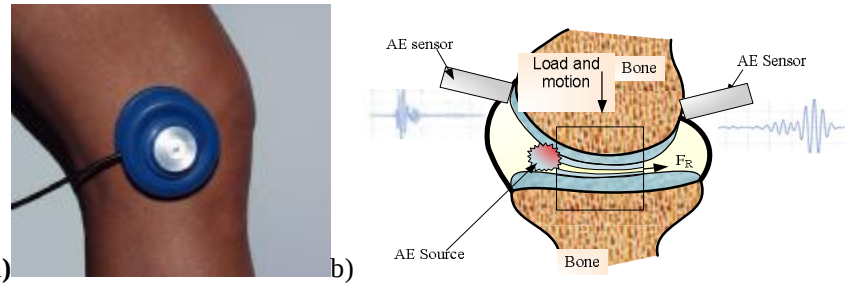

Fig.3. a)Application of an acoustic emission transducer at a human knee joint. b) Principle of location of defects in articular human joint cartilage by using two AE sensors.

To obtain real values of friction forces we must know real values of joint gap height and geometrical structure of cartilage surfaces.

Three various types of defects can be identified during the field test. The acoustic emission caused by cartilage deformation of a healthy knee joint after a sudden change from a two-legs stand- up position to an one-leg stand-up position, is presented in (Fig.3c).

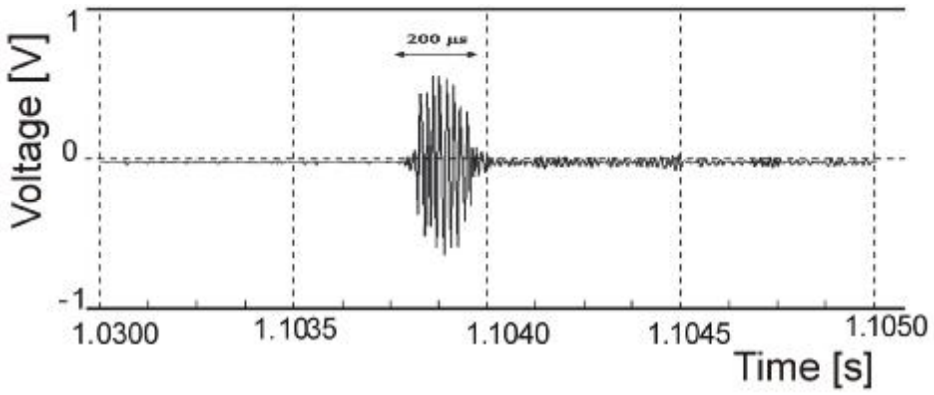

Fig.3c. Acoustic emission signal caused by cartilage deformation of a healthy knee joint after a sudden change from a two-leg stand- up position to a one-leg stand –up position (after Manthei).

The acoustic emission signal generated by a known cartilage lesion is shown in Fig.3d The signal can be split into two regions. Region 1 of small amplitudes was caused by sliding two cartilage surfaces onto the slightly sloping edge of the lesion (1st curve) and on the edge with small visco-elastic deformations (2nd curve). Much greater amplitudes of signals appear in Region 2, caused by sliding out of the lesion from its steep edge (1st curve), and when departing the lesion with the large visco-elastic deformations (2nd curve). These effects are connected with acoustic emission signals of a high rise values, representing both the sequence of motion and the deformation process of the cartilage. The acoustic emission activity process caused by an arthritic defect is presented in Fig.3e, and Fig.3f. In Fig.3e the first and second region shows signals during the entry into the lesion and exit from the lesion on the side of its steep edge in both cases (curve 1). The edge of the lesion for large visco-elastic deformation are showed in curve 2. In Fig.3f the first region shows no signal because the cartilage has no lesion (curve 1). The entry into the second region generates large signals because we have the steep edge of the lesion ,whereas the exit from the second region occurs on the side of the slightly sloping edge (curve 1). Curve 2 shows the large visco-elastic deformations on the side of the entry into the lesion and the exit from the lesion of cartilage, as well.

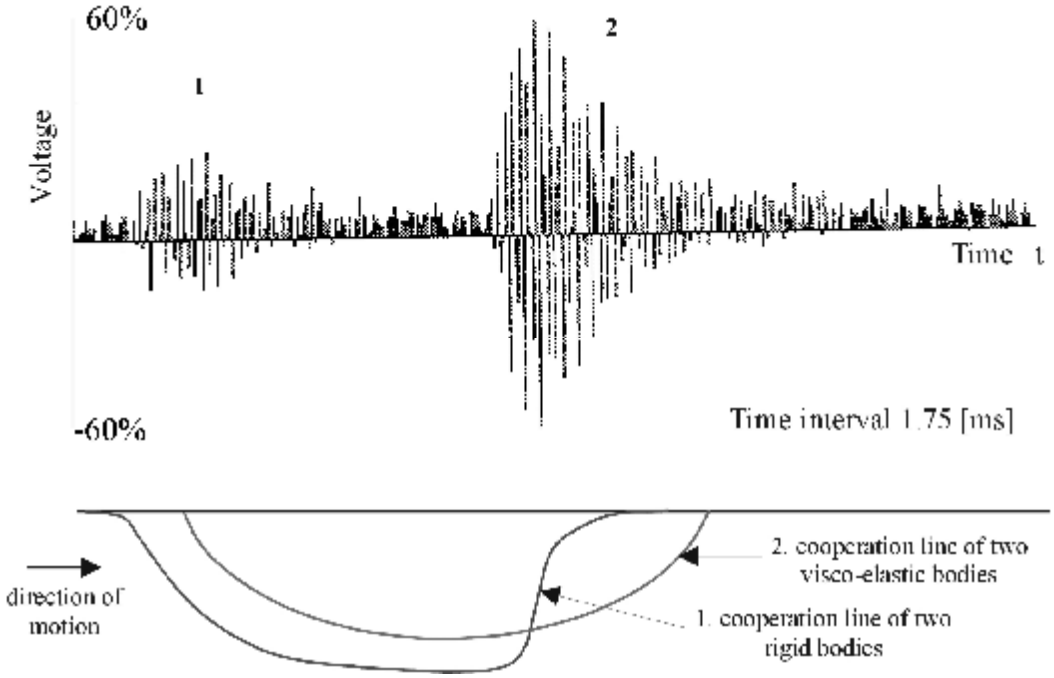

Fig.3d. Acoustic emission signal of a known cartilage lesion: 1st curve shows the sloping edge of the lesion in Region 1 and its steep edge in Region 2, 2nd curve shows small deformations (Region 1) and large visco-elastic deformations (Region 2) (after Manthei).

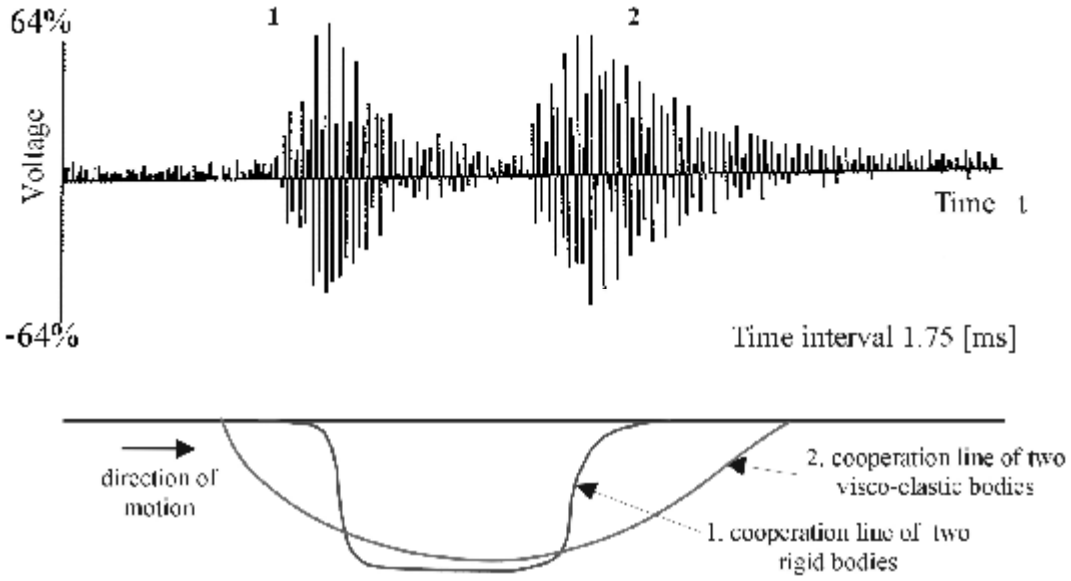

Fig.3e. Acoustic emission signal of an arthritic defect with steep edge on the inlet into the lesion and the steep edge on the outlet from the lesion, see curve 1, and with accompanying large viscoelastic deformations in inlet and outlet the lesion, see curve 2.

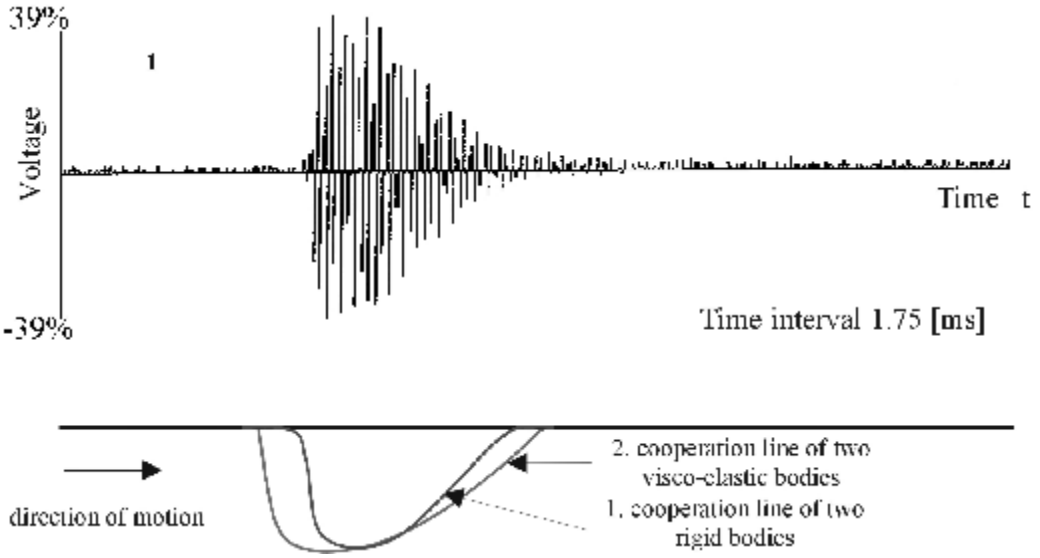

Fig.3f. Acoustic emission signal of a defect of knee joint: Curve 1 for the second region only, with sloping edge on the inlet into the lesion and the steep edge on the outlet from the lesion; Curve 2 shows the large visco-elastic deformations in inlet into the lesion and in outlet from the lesion.

The non-invasive diagnosis is based on the analysis of the acoustic emission caused by day -by- day motion and load in a well defined manner. The advantages of acoustic emission method, compared with those of the established conventional methods (e.g. X ray), are:

- No pain is caused by this procedure.
- This procedure is non-destructive. Mechanical load below the crack initiation threshold is typical for day -by -day life. Therefore for the physiological bone remodeling to avoid degeneration of the bone and joint system is necessary.
- There is no health burden through ionizing irradiation which is unavoidable during X-ray examination.
- There is no danger of infection since this is a non-invasive examination.
- The time necessary for the assessment of the acoustical emission and the data validation analysis is of the order of seconds or minutes at the most.
- The expenses for an acoustic emission measuring system are small as compared with X-ray systems.

3. Friction forces in macro, micro and nano level

During the lubrication the friction forces between two cooperating cartilage surfaces occur in macro-, micro-and nano-scale. The comparison of two bodies cooperating in macro- micro- and nano-scale in human joints is presented in Fig.4a; b; c.

The friction forces in macro- scale are located on the external surfaces of cartilage (see Fig.4a).

The friction forces in micro-scale take place between collagen fibres and between intermediate layers of superficial layer of tissue (see Fig.4b).

The friction forces in nano-scale are tangential to the lateral surfaces of glycoprotein fibres (see Fig.4c). The glycoprotein fibres are of the diameter ranging from *3* to *100 nm*.

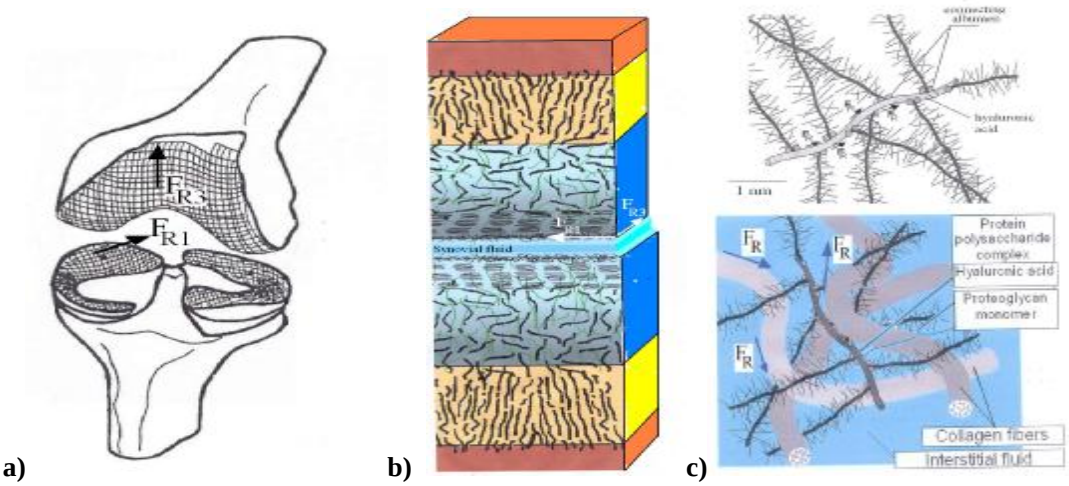

a) **b)** **c)**

Fig.4. a) Macro level friction forces in human joint, b) micro-level friction forces between two cartilage surfaces, c) Protein Polysaccharide Complex and collagen fibres in nano-scale occurring in cartilage layer and friction forces in nano-level scale.

4. Contribution of penetrability of cartilage in liquid solid mechanism on the friction forces

The internal liquid is squeezed out from the superficial layer of cartilage during the joint loading. When the cartilage is more compressed, then it is more difficult a liquid to squeeze out. This fact is presented in Fig.5.

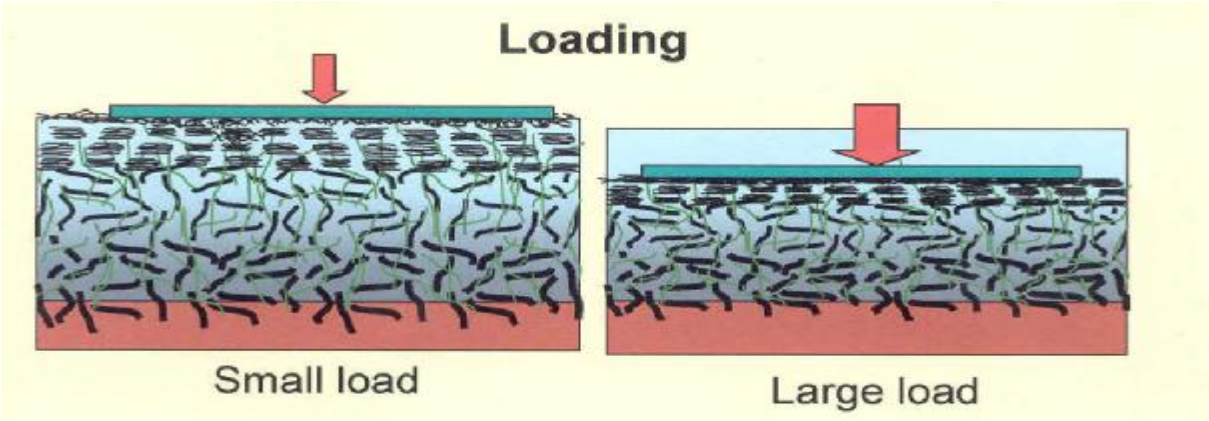

Fig.5. Small and large compression of the superficial layer of cartilage.

The important influence on the friction forces has the penetrability coefficient of cartilage. This coefficient is defined as: c_{por}/η in m^4/Ns where c_{por} denotes the permeability coefficient of porous

cartilage in m^2 and η -denotes dynamic viscosity of synovial fluid. Penetrability coefficient attains the maximum in the same distance from the external surface of the cartilage. The changes of penetrability coefficients along the height of the superficial layer of cartilage is presented in Fig.6. The values of penetrability coefficients of cartilage have values from 2×10^{-16} to $4\times10^{-16}\ m^4/Ns$. If penetrability coefficient decreases, then friction force increases.

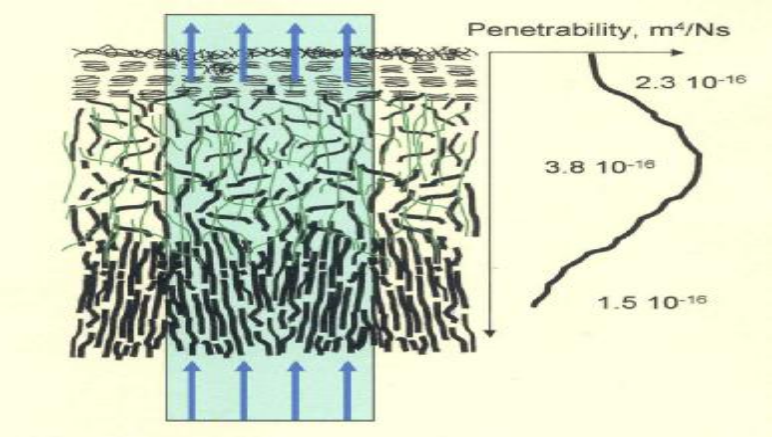

Fig.6. The changes of penetrability coefficients in gap height direction of the thin cartilage layer.

5. Basic equations

Now we take into account the basic equations for unsteady, isotherm flow of biological viscoelastic fluid in boundary layer near to the tissue surface, using Rivlin-Ericksen model. We assume continuity equation and conservation of momentum equation. We show the constitutive stress-strain dependencies of biological nutrient fluids. Such biological fluids contain the additions for example oxygen carrying fluorocarbons and diagnostic substances. These fluids have usually non-Newtonian properties. The non-Newtonian properties mark the non-linear dependencies between strain and stress relations. The dynamic viscosity or apparent dynamic viscosity of biological liquids with nutrition and other additions often decreases with increasing of shear rate during the motion. Biological liquids with nutrition and fluorocarbons have mostly pseudoplastic, or micro-polar properties, which are caused by the small elastic additions of fluorocarbons and other elastic particles. Necessary values of pseudo-viscosity coefficients occurring in stress-strain relations for biological fluids are obtained in experimental way and afterwards are used in the numerical calculations.

6. Beaver's boundary conditions for the flow in biobearing gap

The boundary conditions for the unknown synovial fluid velocity components caused by rotational motion in the circumferential direction φ and squeezing have the known classical form (Wierzcholski, 2005a; b; c; d; f; Wierzcholski and Cwanek, 2005e). In the case of permeable cartilage surface we additionally take into account the Beaver's boundary conditions (Beavers *et al.*, 1970; Cieszko and Kubik, 1999). The graphical form of the Beaver's boundary conditions is presented in Fig.7.

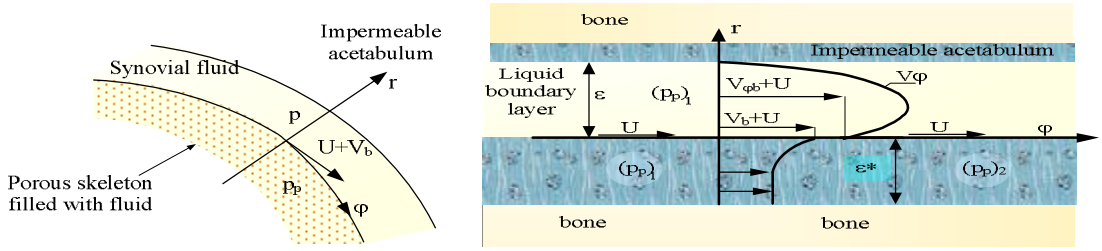

Fig.7. Boundary conditions for synovial fluid circumferential velocity component in thin layer resting on the movable and permeable porous cartilage, where r denotes gap height direction: a) acetabulum, joint gap and bone head, b) model of the boundary condition.

Porous permeable cartilage lies on the bone head. The peripheral velocity of the bone head is $U = \omega R$ (Mow and Guilak, 1994).

We introduce the following symbols: ω - the angular velocity of the bone in the circumferential direction φ. The value of the height of the human joint gap is $\varepsilon \approx 2 \cdot 10^{-5} m$. The pressure in pores is p_p. The symbol p denotes hydrodynamic pressure.

The unknown velocity component is obtained from the following boundary conditions (Cieszko and Kubik, 1999)

$$v_\varphi = 0 \qquad \text{for} \qquad r = \varepsilon, \tag{6.1}$$

$$v_\varphi = v_{\varphi b} + U \qquad \text{for} \qquad r = 0, \tag{6.2}$$

$$\frac{dv_\varphi}{dr} = \frac{c_\alpha}{\sqrt{c_{por}}}\left(v_{\varphi b} - V_b\right) \qquad \text{for} \qquad r = 0, \tag{6.3}$$

$$V_b = -\frac{c_{por}}{\eta c_\lambda}\frac{\partial p_p}{\partial \varphi}. \tag{6.4}$$

The pressure in pores p_p produces the velocity V_b in the horizontal (or circumferential) direction. To determine the unknown value of the velocity $v_{\varphi b}$ we use the boundary Beavers condition (6.3). The symbol c_{por} $(in\ m^2)$ stands for the permeability coefficient of the porous cartilage. The dimensionless coefficient c_α depends on the degree of the cartilage surface porosity.

7. Beaver's boundary conditions for the flow in cartilage canals and friction forces

The boundary condition for the liquid flow through the porous canal in the superficial layer of cartilage in human joint is now determined. We take into account that the canal is limited by the impermeable and permeable walls of cartilage. After Darcy and Beavers investigations, the liquid velocity component v_φ can be determined by the following equation (Beavers *et al.*, 1970; Cieszko and Kubik, 1999).

$$\frac{\partial^2 v_\varphi}{\partial r^2} = \frac{1}{\eta}\frac{\partial p_p}{c_\lambda \partial \varphi} \tag{7.1}$$

where $0 \le r \le \varepsilon_{ch}$ and ε_{ch} is the height of the channel in porous tissue. In this liquid the flow in boundary layer depends only on the pressure in pore, p_p. The horizontal axis (φ) lies on the lower surface and the vertical axis (r) is perpendicular to the height of the canal gap (see Fig.8.a, b, c). The symbol c_λ denotes dimensional value of channel length.

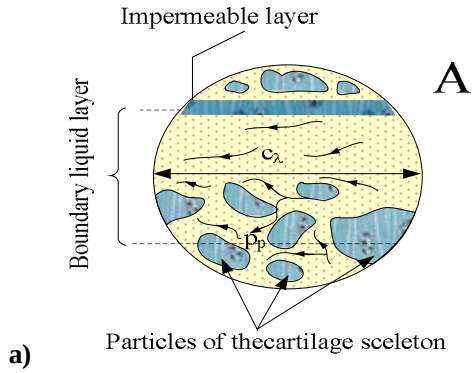

a)

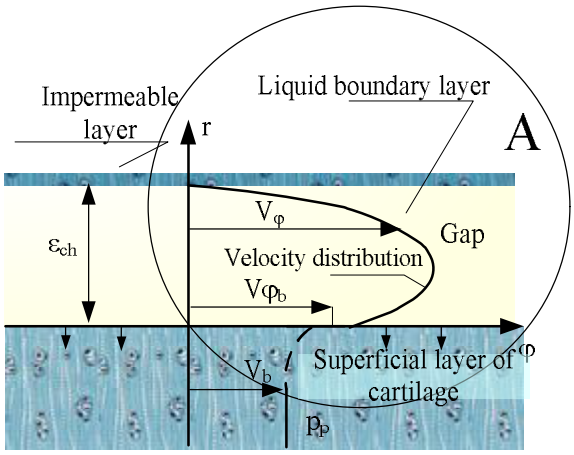

b)

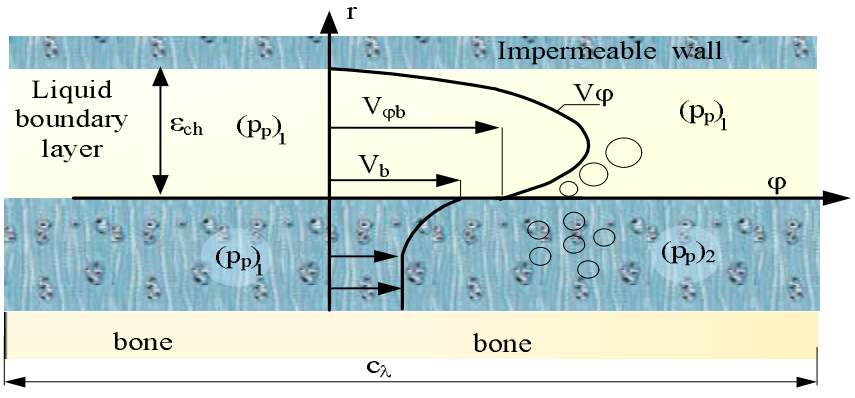

c)

Fig.8. Boundary conditions for the liquid velocity distribution in the porous canal within cartilage at $(p_p)_1 > (p_p)_2$: a) canal in porous tissue, b) model of the canal c) velocity distribution in the porous canal.

If the boundary layer of viscous liquid is limited by the permeable porous superficial layer on the lower surface and by the impermeable tissue laying on the upper surface, then the boundary conditions for the velocity component in φ-direction have the following form

$$v_{\varphi} = 0 \qquad \text{for} \qquad r = \varepsilon_{ch}, \tag{7.2}$$

$$v_{\varphi} = v_{\varphi b} \qquad \text{for} \qquad r = 0, \tag{7.3}$$

$$\frac{dv_{\varphi}}{dr} = \frac{c_{\alpha}}{\sqrt{c_{por}}}\left(v_{\varphi b} + \frac{c_{por}}{\eta c_{\lambda}} \frac{\partial p_p}{\partial \varphi} \right), \qquad \text{for} \qquad r = 0. \tag{7.4}$$

We can use the Beavers condition (7.4) to determine the unknown value of the tangential velocity $v_{\varphi b}$ on the permeable cartilage surface in the point $r = 0$. This condition determines the angle of inclination of the velocity trajectory on the permeable surface.

The flow of the liquid through the canal depends only on the pressure in pores. The dimensionless value c_{α} and velocity $v_{\varphi b}$ have been already determined above.

The friction forces in φ, ϑ directions have the following forms

$$F_{R1\varphi} = \iint_{\Omega} \left(\eta \frac{\partial v_{\varphi}}{\partial r} \right)_{r=\varepsilon_{ch}} d\Omega, \qquad F_{R3\vartheta} = \iint_{\Omega} \left(\eta \frac{\partial v_{\vartheta}}{\partial r} \right)_{r=\varepsilon_{ch}} d\Omega \tag{7.5}$$

where: v_{φ} - synovial fluid velocity component in the circumferential φ direction, v_{ϑ} - synovial fluid velocity component in meridional direction ϑ in spherical coordinates, η - dynamic viscosity of synovial fluid, ε_{ch} - dimensional height of the channel in porous cartilage, Ω - dimensional value of lubrication area. The solution of the Eq.(7.1) under the boundary conditions (7.2), (7.3), (7.4) gives the following solution of the liquid velocity component in φ direction, inside the canal for $0 \le r \le \varepsilon_{ch}$

$$v_{\varphi} = v_{\varphi b}\left(1 + \frac{c_{\alpha}}{\sqrt{c_{por}}} r \right) + \frac{1}{2\eta}\left(r^2 + 2c_{\alpha} r \sqrt{c_{por}} \right) \frac{dp_p}{c_{\lambda} d\varphi} = \frac{dp_p}{c_{\lambda} d\varphi} \frac{\sqrt{c_{por}}\left(r^2 - \varepsilon_{ch}^2 \right) + c_{\alpha}\left(\varepsilon_{ch} r + 2c_{por} \right)\left(r - \varepsilon_{ch} \right)}{2\eta\left(\sqrt{c_{por}} + c_{\alpha}\varepsilon_{ch} \right)} \tag{7.6}$$

where

$$v_{\varphi b} = -\frac{c_{por}}{2\eta}\left(\frac{c_{\sigma}^2 + 2c_{\alpha}c_{\sigma}}{1 + c_{\alpha}c_{\sigma}} \right) \frac{dp_p}{c_{\lambda} d\varphi}, \tag{7.7}$$

$$c_{\sigma} \equiv \frac{\varepsilon_{ch}}{\sqrt{c_{por}}}. \tag{7.8}$$

Figure 8 shows the parabolic distribution of nutrient liquid velocity in the boundary layer inside the canal in porous tissue. Taking into account the component of liquid velocity Eq.(7.6), we can obtain the friction forces friction forces produced by liquid flow in canal in the following form

$$F_{R\varphi} = \iint_{\Omega}\left(\eta\frac{\partial v_{\varphi}}{\partial r}\right)_{r=\varepsilon_{ch}} d\Omega = \frac{2\varepsilon_{ch}\sqrt{c_{por}} + c_{\alpha}\varepsilon_{ch}^{2} + 2c_{\alpha}c_{por}}{2c_{\lambda}\left(\sqrt{c_{por}} + c_{\alpha}\varepsilon_{ch}\right)} \iint_{\Omega}\frac{dp_{p}}{d\varphi} d\Omega.. \tag{7.9}$$

8. Conclusions

In this paper are presented the analytical solutions of various kinds of the friction forces occurring in of human joints gap and in pores of cartilage joint caused by: hydrodynamic lubrication by rotation, by squeezing, boosted squeezing and weeping. Permeable phenomena of the synovial fluid inside cartilage pores are taken into account.

Acknowledgment

This research project has been supported by a Marie Curie Transfer of Knowledge Fellowship of the European Community`s Sixth Framework Program under contract number MTKD-CT-2004-517226.

References

Ahn H.-S., Chizhik S.A., Dubravin A.M., Kazachenko V.P. and Popov V.V. (2001): *Application of phase contrast imaging atomic force microscopy to tribofilms on DLC coatings.* – Wear, vol.249, pp.617-625.

Beavers G.S., Sparrow E.M. and Magnuson R.A. (1970): *Experiments on coupled parallel flows in a channel and bounding porous medium.* – Journal of Basic Engineering, pp.843-848.

Cieszko M. and Kubik J. (1999): *Derivation of matching conditions at the contact surface between fluid-saturated porous solid and bulk fluid.* – Transport in Porous Media, vol.34, pp.319-336.

Chizhik S.A., Huang Z., Gorbunov V.V., Myshkin N.K. and Tsukruk V.V. (1998): *Micromechanical properties of elastic polymeric materials as probed by scanning force microscopy.* – Langmuir, vol.14, pp.2606-2609.

Chizhik S.A., Ahn H.-S., Chizhik V.V. and Suslov A.A. (2004): *Tuning fork energy dissipation nanotribometry as option of AFM.* – Proceeding International Workshop "Scanning Probe Microscopy", Nizhny Novgorod, pp.119-121.

Dowson D. (1990): *Bio-Tribology of Natural and Replacement Synovial Joints.* In: Van Mow C., Ratcliffe A., Woo S.L-Y.: Biomechanics of Diarthrodial Joint. – New York, Berlin, Londyn, Paris, Tokyo, Hong Kong: Springer-Verlag, vol.2.

Fink F. And Manthei G. (2004): *Gedanken zur nahfeldeffekten bei der signal-basierten schallemissios-analyse.* – Otto-Graf-Journal der Universität Stuttgard, vol.15, pp.121-134.

Manthei G. (2006): *Implementation of Acoustic Emission Method: Fundamentals and Applications for Biobearings.* – Transfer of Knowledge Development, MTKD –CT-2004-517226.

Mow V.C., Holmes M.H. and Lai W.M. (1984): *Fluid transport and mechanical properties of articular cartilage*. – Journal of Biomechanics, vol.17, pp.337-394.

Mow V.C., Ratcliffe A. and Woo S. (1990): *Biomechanics of Diarthrodial Joints.* – Berlin, Heidelberg, New York: Springer Verlag.

Mow V.C. and Soslowsky L.J. (1991): *Friction, lubrication and wear of diarthrodial joints*. In: Mow VC, Hayes WC, eds. – Basic Orthopedic Biomechanics. New York: Raven Press, pp.254-291.

Mow V.C. and Guilak F. (1994): *Cell Mechanics and Cellular Engineering.* – Berlin, Heidelberg, New York: Springer Verlag.

Sieroń A. (2000): *Applications of magnetic fields in medicine* (In Polish). – Bielsko Biała, Alfa Medica Press.

Wierzcholski K. (2005a): ***Random changes of temperature in slide bearing gap.*** – International Congress Thermal Stress IUTAM Proceedings, Vienna, 2005, pp.449-452.

Wierzcholski K. (2005b): ***Intelligent artificial joint and regeneration problems in articular joints***. – Journal of Kones International Combustion Engines, Warsaw, vol.12, No.3-4, pp.355-362.

Wierzcholski K. (2005c): ***Stochastic non-isothermic lubrication of hip joint with deformable cartilage***. – Tribologia, 4/2005, vol.202, pp.309-322.

Wierzcholski K. (2005d): *Импульсная смазка в тазобедренном суставе для гипоупругой модели хряща.* – Российский Журналоf Биомеханики Perm, vol.9, No.2, pp.42-63.

Wierzcholski K. and Cwanek J. (2005e): ***Measurements of surface roughness of heads of human hip joints in lubrication aspects.*** – Zeszyty Naukowe Katedry Mechaniki Stosowanej Technical University of Gliwice, pp.477-483.

Wierzcholski K. (2005f): ***Asperities and deformations of hyper elastic joint cartilages in cultivation aspects*** (in English). – Zeszyty Naukowe Katedry Mechaniki Stosowanej Technical University of Gliwice, pp.469-475.

Received: May 19, 2006

Revised: August 2, 2006